SUPPLEMENTAL INFORMATION

Kinetic Phases of Ag-Cu Alloy Films are Accessible through Photodeposition

Kevan E. Dettelbach,[a] Jingfu He,[a] Noah J. J. Johnson[a] Aoxue Huang,[a] Adam Bottomley,[a] Brian Lam,[a] Danielle A. Salvatore,[b] Curtis P. Berlinguette[a,b,c*]

[a]Department of Chemistry, The University of British Columbia, 2036 Main Mall, Vancouver, BC V6T1Z1.
[b]Department of Chemical & Biological Engineering, The University of British Columbia, 2360 East Mall, Vancouver, BC V6T1Z3.
[c]Stewart Blusson Quantum Matter Institute, The University of British Columbia, 2355 East Mall, Vancouver, BC V6T1Z4.

[*]Correspondence to: cberling@chem.ubc.ca (CPB)

Contents:

Table S1. Elemental Analysis for a Series of Ag-Cu Films.

Sample[a]	EDX Mapping[b]	
	% Ag	% Cu
Ag0.9Cu0.1	90 ± 3	10 ± 3
Ag0.5Cu0.5	47 ± 4	53 ± 4
Ag0.1Cu0.9	16 ± 1	84 ± 1

[a]The nomenclature used in this table and the Supporting Information is as follows: Films denoted **Ag*x*Cu1-*x*** are those derived from the relative molar proportions of the respective metals in the precursor solutions (x = 0.9, 0.5, and 0.1); monometallic films are denoted **Ag** and **Cu**.

[b]Energy dispersive X-ray spectroscopic elemental mapping data was collected using a FEI Helios NanoLab 650 dual beam scanning electron microscope with an EDAX Pegasus system. The values shown were averaged from three different locations and the error was calculated using the root-mean-square error method.

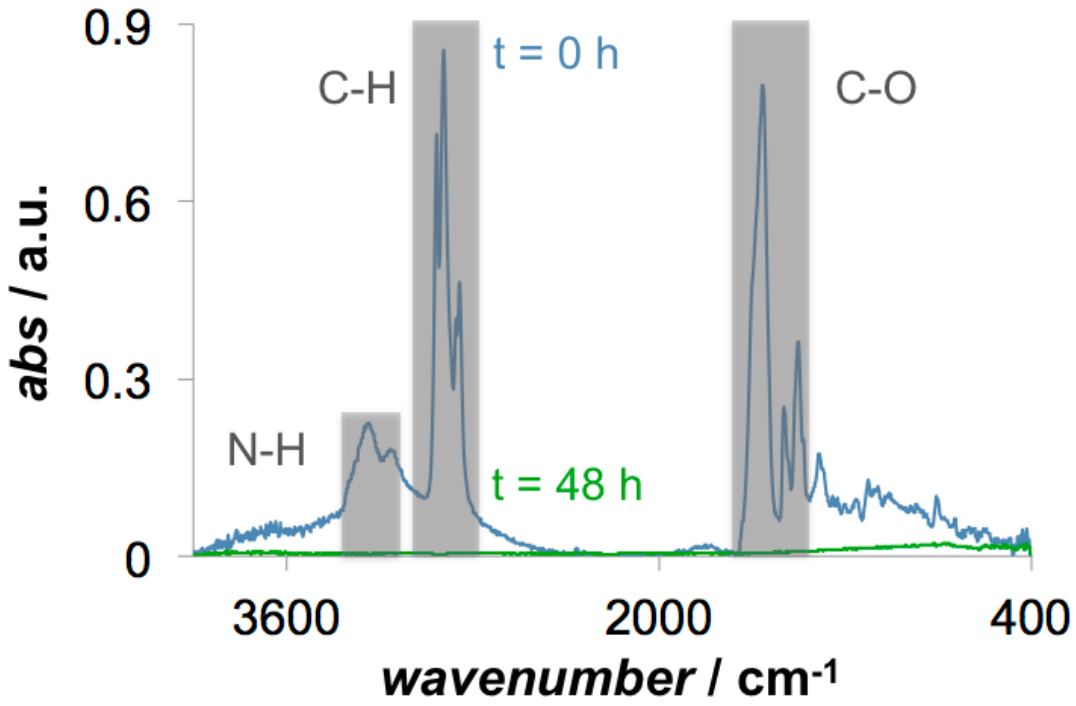

Figure S1. FTIR spectrographs recorded before (blue) and after (green) photolysis of the precursor film used to prepare **Ag0.9Cu0.1**. The N-H, C-H, and C-O vibrational modes are all absent in the photolyzed films.

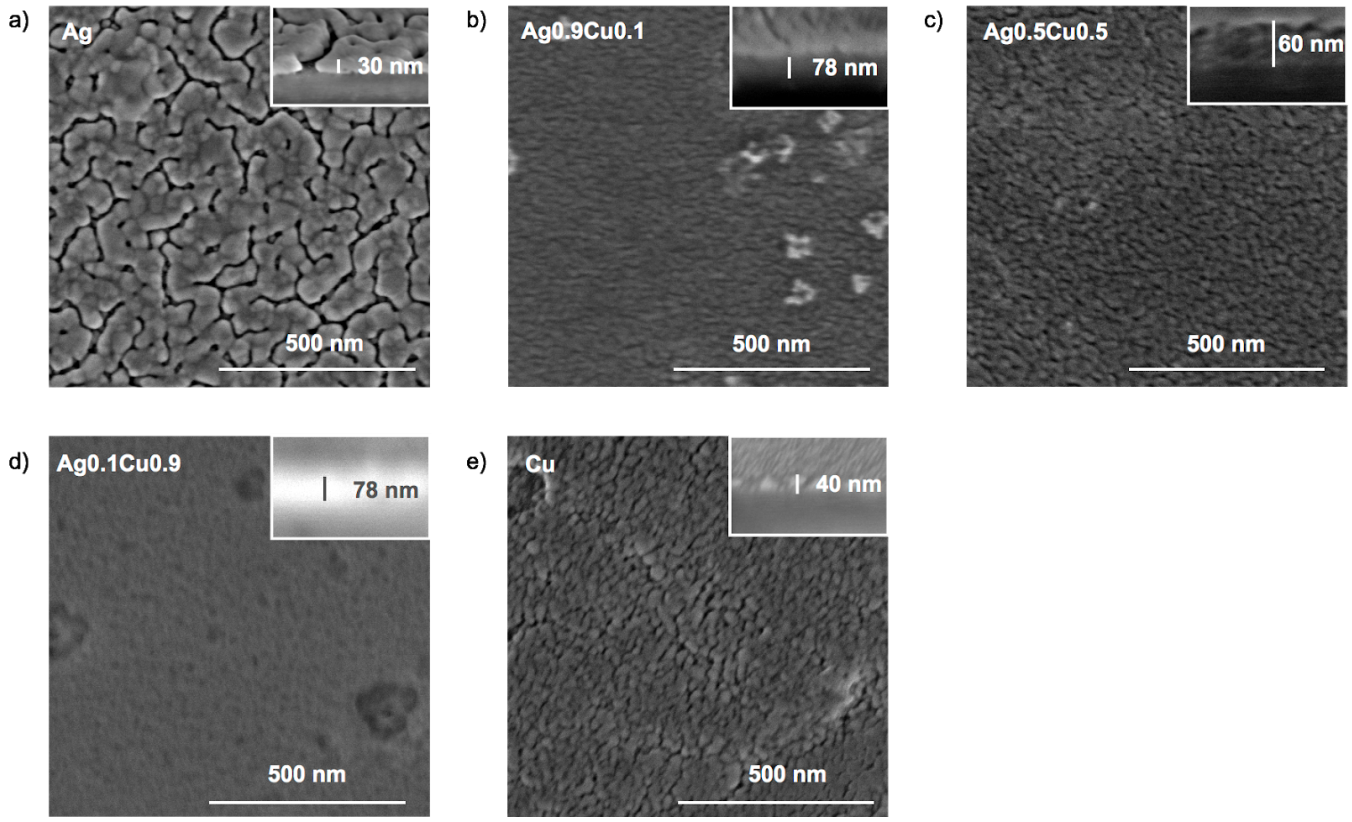

Figure S2. SEM images of a) **Ag**, b) **Ag0.9Cu0.1**, c) **Ag0.5Cu0.5**, d) **Ag0.1Cu0.9**, and e) **Cu**. *Inset*: Cross-sections of films show thicknesses of the title materials to be 30-80 nm. The cross sections were created by etching the films with a focused ion beam on its lowest current setting (1 pA). (The sample names for the Ag-Cu films refer to the relative metal stoichiometry of the precursor solutions and not the alloys; see footnote of Table S1.)

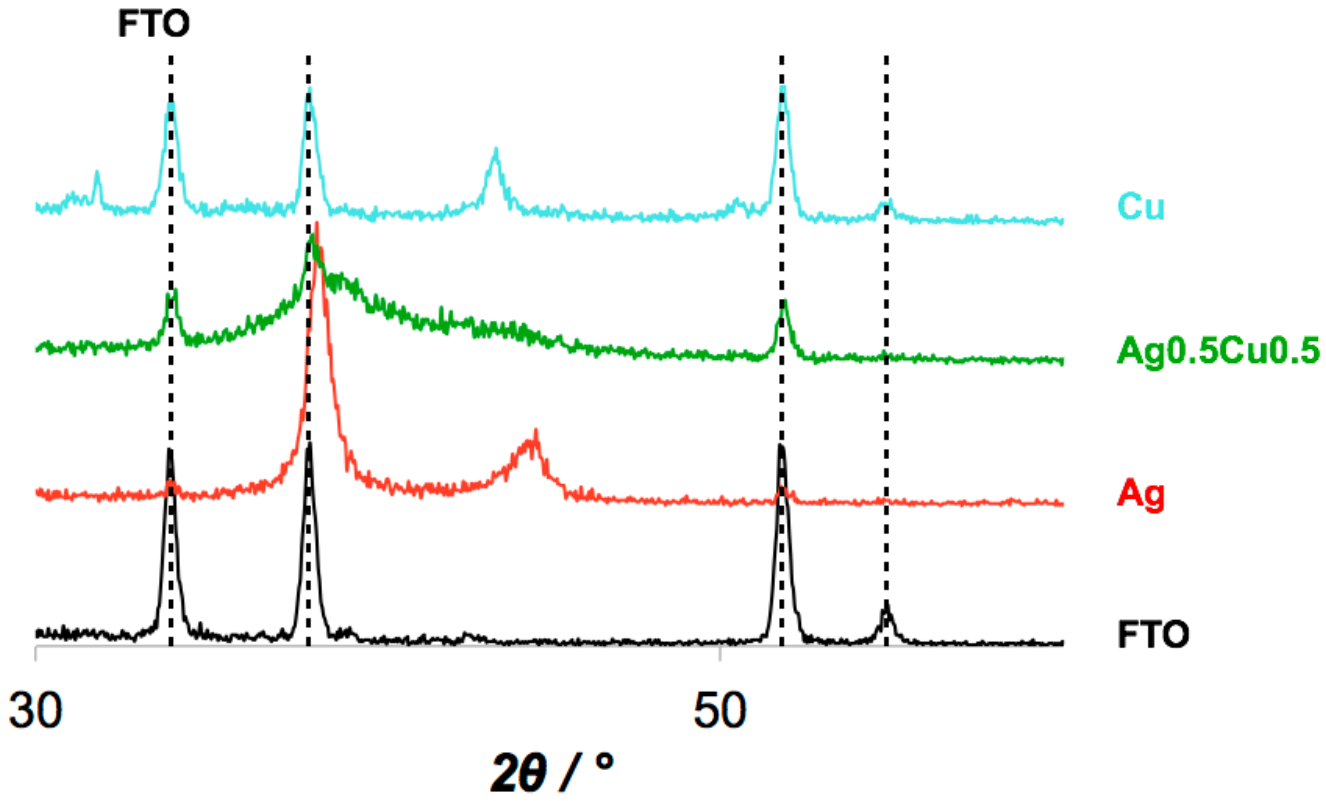

Figure S3. Grazing incidence X-ray diffractograms for films deposited on FTO. Data for bare FTO is also provided for reference. The FTO peaks are aligned for all samples to rule out any peak shifting due to instrumental or alignment issues. The vertical dashed lines show the locations of peaks in the bare FTO sample. (The sample names for the Ag-Cu films refer to the relative metal stoichiometry of the precursor solutions and not the alloys; see footnote of Table S1.)

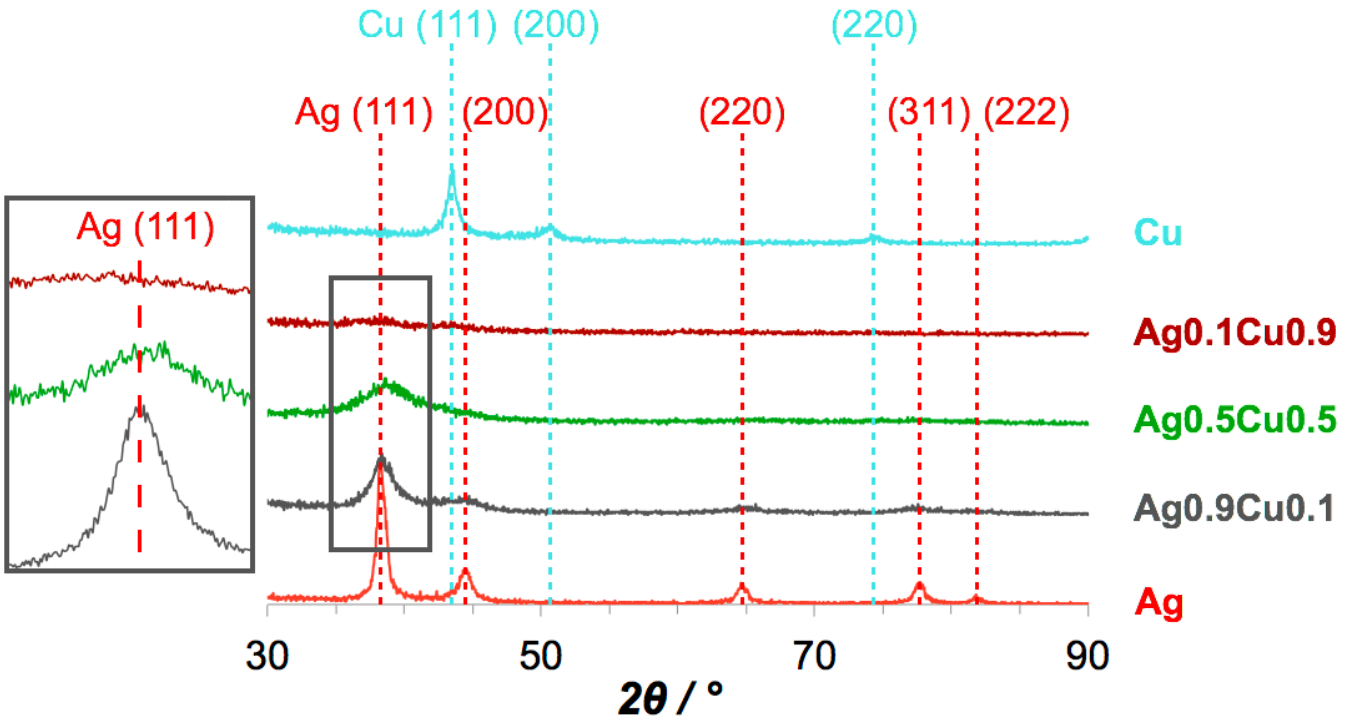

Figure S4. Grazing incidence X-ray diffractograms for **Ag**, **Ag0.9Cu0.1**, **Ag0.5Cu0.5**, **Ag0.1Cu0.9**, and **Cu** samples. Measurements were taken with an incident angle of 0.3°and a scan rate of 2.5 ° min^{-1}. Inset: detail scan of the Ag (111) region with a scan rate of 0.5 ° min^{-1}. Increasing Cu content results in slightly different Ag phases for the **Ag0.9Cu0.1**, and **Ag0.5Cu0.5** compositions as indicated by the shift in the Ag (111) peak. No Ag (111) peak is discernible for the **Ag0.1Cu0.9** sample. Ag and Cu reference lines are from the peaks in the Ag and Cu control films and were assigned based on pdf number 04-0783 and pdf number 04-0836, respectively. (The sample names for the Ag-Cu films refer to the relative metal stoichiometry of the precursor solutions and not the alloys; see footnote of Table S1.)

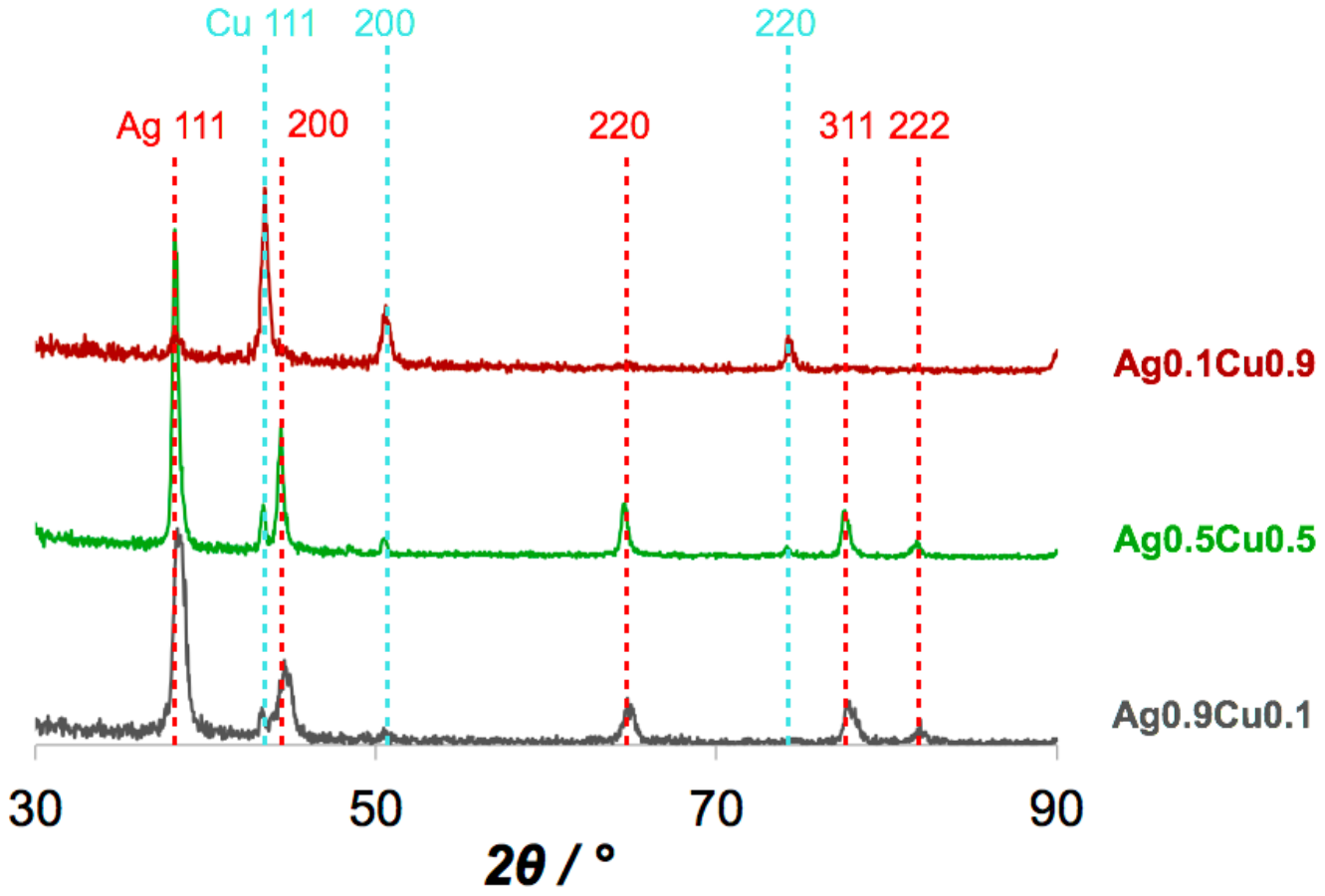

Figure S5. Grazing incidence X-ray diffractograms for Ag-Cu films annealed at 200 °C under an N_2 atmosphere confirm phase separation for all compositions. Ag and Cu reference lines are from the peaks in the Ag and Cu control films and were assigned based on pdf number 04-0783 and pdf number 04-0836, respectively. (The sample names for the Ag-Cu films refer to the relative metal stoichiometry of the precursor solutions and not the alloys; see footnote of Table S1.)

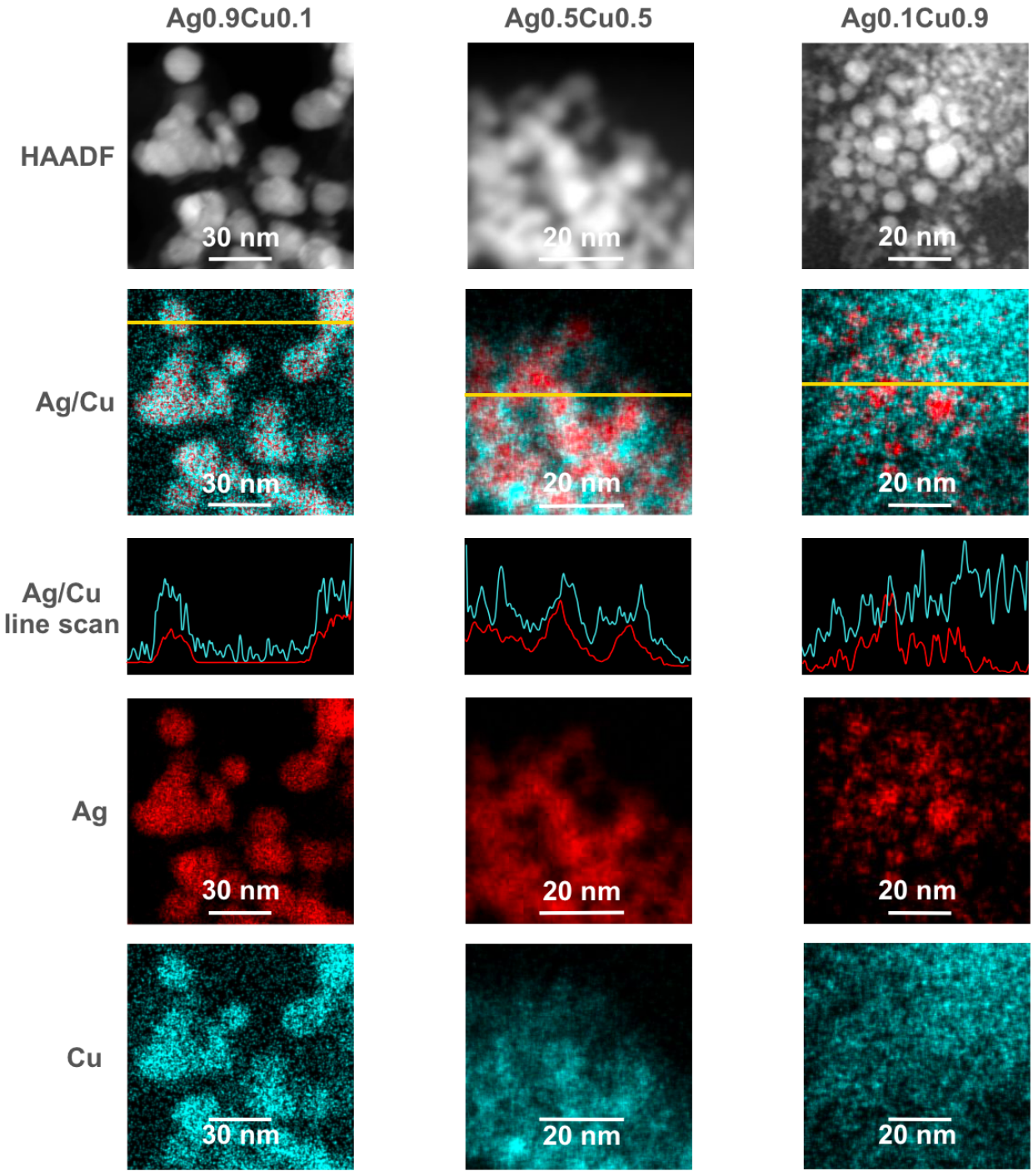

Figure S6. STEM EDX elemental mapping of the **Ag0.9Cu0.1**, **Ag0.5Cu0.5,** and **Ag0.1Cu0.9** films showing Ag (red) and Cu (blue) distributions as well as the high angle annular dark field images (HAADF). The yellow line shows where the line scans were calculated. Mapping for the **Ag0.9Cu0.1** film shows that Ag and Cu are uniformly distributed within the nanoparticles. The **Ag0.5Cu0.5** data indicates both Ag and Cu within the nanoparticles, but with a higher concentration of Ag at the core of the particles. The **Ag0.1Cu0.9** data shows phase segregation with Ag being confined to the larger nanoparticles on top of a field of smaller Cu particles. (The sample names for the Ag-Cu films refer to the relative metal stoichiometry of the precursor solutions and not the alloys; see footnote of Table S1.)

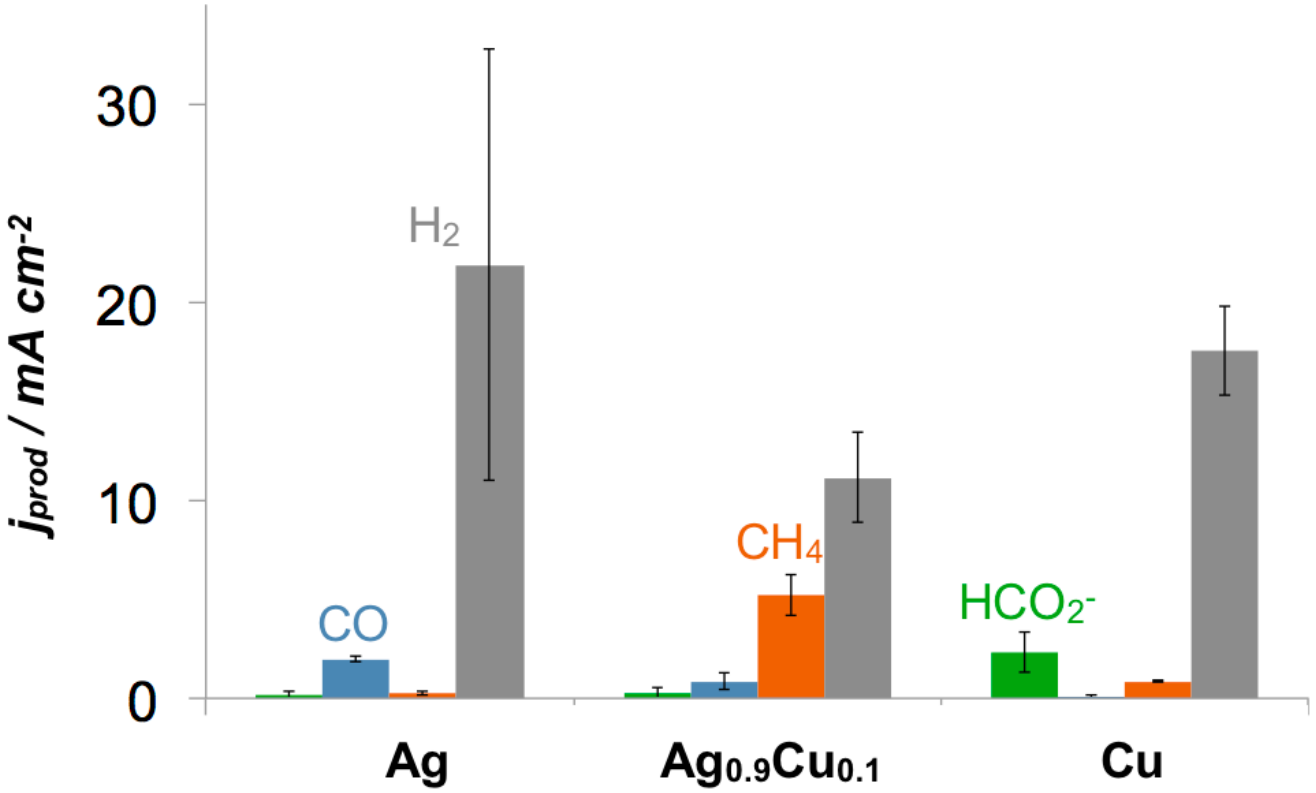

Figure S7. Partial current densities for CO (blue), CH_4 (orange), HCO_2^- (green) and H_2 (gray) mediated by the $Ag_{0.9}Cu_{0.1}$ alloy as well as silver and copper control films. The films were deposited onto glassy carbon. The data was obtained at a potential of -1.75 V vs RHE. All electrochemical tests were conducted in a 0.25-M K_2CO_3 electrolyte.

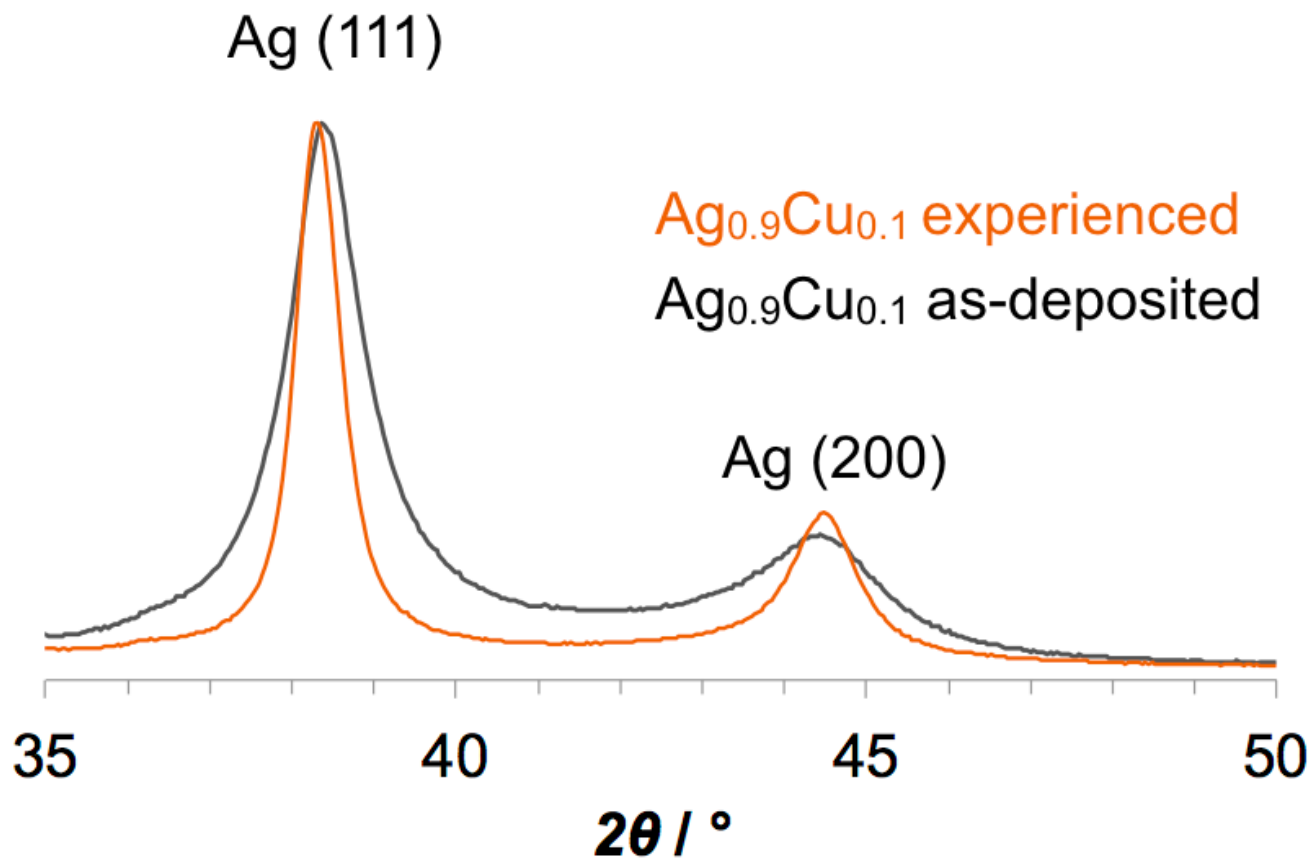

Figure S8. Grazing incidence X-ray diffractograms for the $Ag_{0.9}Cu_{0.1}$ film on glassy carbon after performing CO_2 reduction for 0.5 h at -1.75 V vs RHE. We refer to this film as "experienced". The as-deposited film is shown for reference. Both traces have been normalized with respect to intensity. The experienced $Ag_{0.9}Cu_{0.1}$ film displays peaks with the same phase as the as-deposited film. The peaks are narrower in the experienced film likely due to an increase in the size of the crystallites. There is no evidence of phase separation. The Ag (111) and Ag (200) peaks were assigned based on pdf number 04-0783.

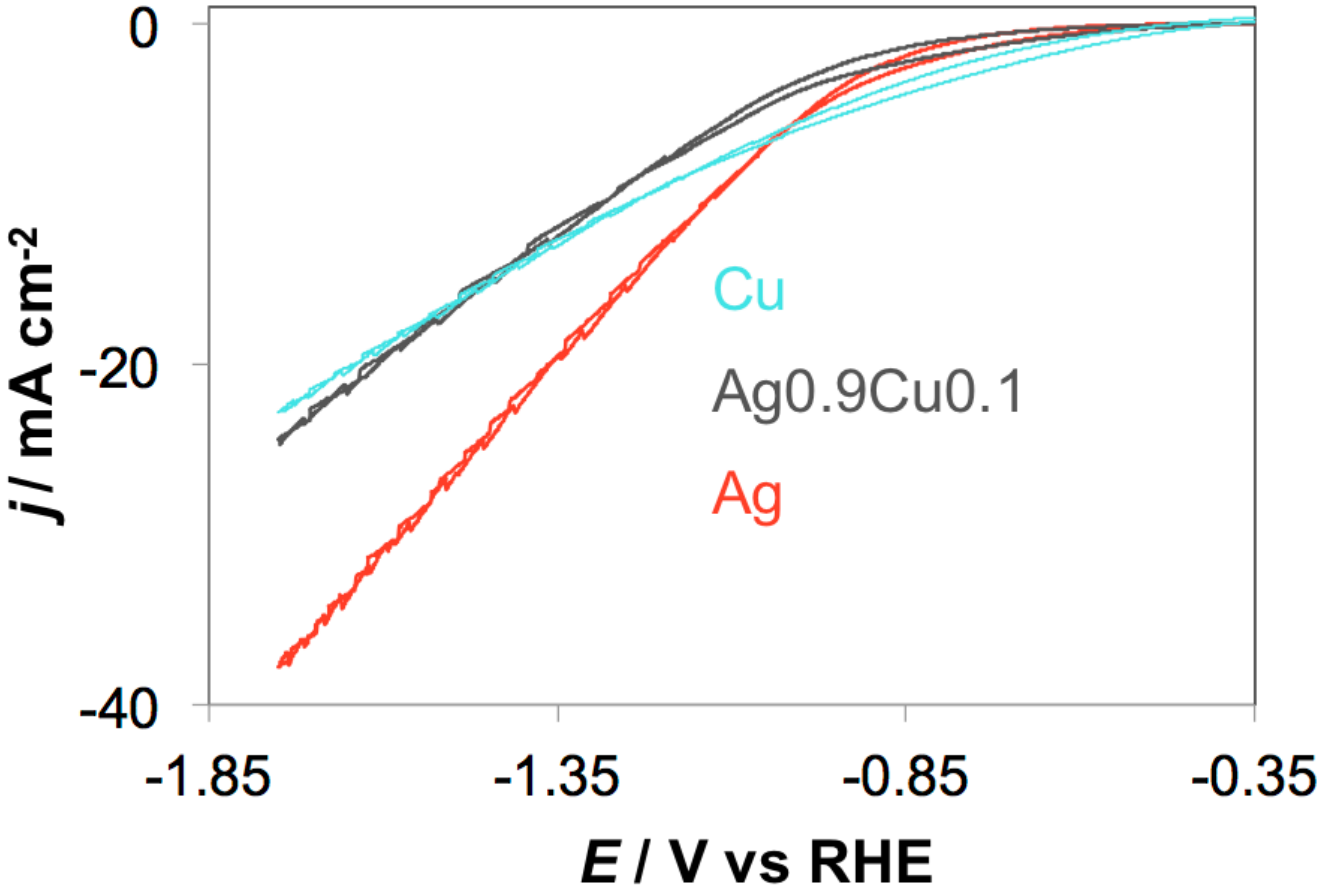

Figure S9. Cyclic voltammograms for the $Ag_{0.9}Cu_{0.1}$ alloy (gray) and the silver (red) and copper (blue) control films. All films were deposited onto glassy carbon. Potentials are reported vs RHE and all scans were performed in 0.25-M K_2CO_3 electrolyte at a scan rate of 0.01 V s^{-1}.